Domain Wall Color Code

Konstantin Tiurev [1,*] Arthur Pesah, [2] Peter-Jan H. S. Derks, [3] Joschka Roffe, [3,4]
Jens Eisert, [3,5] Markus S. Kesselring, [3] and Jan-Michael Reiner [1]

[1] *HQS Quantum Simulations GmbH, Rintheimer Strasse 23, 76131 Karlsruhe, Germany*
[2] *Department of Physics and Astronomy, University College London, London WC1E 6BT, United Kingdom*
[3] *Dahlem Center for Complex Quantum Systems, Freie Universität Berlin, 14195 Berlin, Germany*
[4] *Quantum Software Lab, University of Edinburgh, Edinburgh EH8 9AB, United Kingdom*
[5] *Helmholtz-Zentrum Berlin für Materialien und Energie, 14109 Berlin, Germany*

We introduce the domain wall color code, a new variant of the quantum error-correcting color code that exhibits exceptionally high code-capacity error thresholds for qubits subject to biased noise. In the infinite bias regime, a two-dimensional color code decouples into a series of repetition codes, resulting in an error-correcting threshold of 50%. Interestingly, at finite bias, our color code demonstrates thresholds identical to those of the noise-tailored XZZX surface code for all single-qubit Pauli noise channels. The design principle of the code is that it introduces domain walls which permute the code's excitations upon domain crossing. For practical implementation, we supplement the domain wall code with a scalable restriction decoder based on a matching algorithm. The proposed code is identified as a comparably resource-efficient quantum error-correcting code highly suitable for realistic noise.

Quantum computers hold the promise to solve certain classes of computational problems with exponential speed-ups over the best known classical algorithms [1]. To enable large-scale quantum computations, information must be stored and processed in a nearly noiseless fashion. However, all components of the quantum computer, including physical qubits, gate operations, and measurements, are inevitably prone to errors. Fragile quantum information can be protected by countering errors with quantum error-correcting codes (QECCs), albeit at substantial resource overheads [2–5]. Such codes turn a collection of noisy, physical qubits into a more robust logical qubit by redundantly encoding information in a nonlocal way. Provided the physical qubit noise is below a certain threshold, the logical error rate can be made arbitrarily small by increasing the number of physical qubits in the code [6,7]. The challenge of practical error correction is to design codes that admit sufficiently high error thresholds and use a reasonable number of physical qubits to achieve the desired logical failure rates. Optimizing these figures of merit has been the core subject of research in the field of quantum error correction.

Among the diverse range of QECCs, topological surface [8–11] and color codes [12–15] are of special interest for practical purposes since they require only geometrically local operations on a two-dimensional qubit layout and exhibit remarkable abilities to protect quantum information. The color code is especially appealing as it supports the transversal implementation of the full Clifford gate set [12,16,17], such that single-qubit errors do not propagate to the remaining qubits of the code when logical gates are executed [18,19]. Furthermore, the three-dimensional color code supports transversal non-Clifford gates [15,17,20], which, in conjunction with a technique called code switching [17,21,22], paves the way to a universal set of fault-tolerant gates. Finally, the color code requires smaller resource overhead to encode a logical qubit compared to the surface code of the same distance [23–28].

The ability of a code to detect and correct errors strongly depends on the structure of noise affecting qubits on the physical level. Practical error correction strategies have to be tailored to properties of realistic noise, such as the common situation where noise is biased towards a diagonal Pauli channel, e.g., dephasing. Such noise regimes are common in many hardware architectures, including superconducting qubits [29,30], trapped ions [31], and quantum dots [32]. Certain qubit architectures are purposely designed to exhibit strong bias in their noise characteristics [33,34]. The capability of the standard surface and color codes to correct errors quickly deteriorates for such asymmetric biased-noise channels. The same asymmetry can be exploited to fit the error correction strategy [34–39], resulting in remarkable gains in the code's efficiency. The surface code in its so-called XZZX configuration [35] yields exceptionally high biased-noise thresholds which can match and even exceed the random-code hashing

---

*Contact author: konstantin.tiurev@quantumsimulations.de, konstantin.tiurev@gmail.com
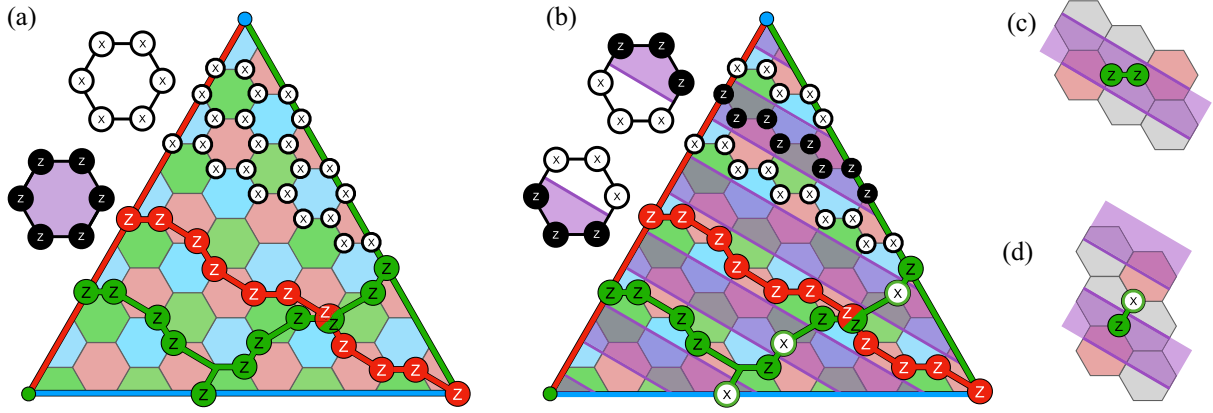
FIG. 1. A distance-11 color code in its (a) CSS and (b) X^3Z^3 configurations. (a) Qubits lie on the vertices of the hexagonal lattice. Each tile corresponds to a primal and a dual stabilizers of Eq. (1). Logical Pauli operators are tensor products of physical Pauli operators acting on qubits supported on non-trivial strings that commute with all stabilizers of the code. Logical operators can be deformed by multiplying them with stabilizers. Two realizations of the logical $\bar{Z}$ operator are shown with the red and green strings of Pauli Zs. Similarly, logical $\bar{X}$ is a product of Pauli Xs supported on the same qubits. Because of the CSS structure of the stabilizers, there exist many possible logical operators composed of only X or only Z Paulis. (b) The X^3Z^3 color code. For convenience, we show primal stabilizers along even diagonals and dual stabilizers along odd diagonals. The stabilizers form domains, where single-qubit Paulis of one type are measured by stabilizers. The domains are separated by DWs (thin purple lines). Anyons of the same color can be paired by single-qubit Pauli errors of one type if they lie within the same domain, as in panel (c). In contrast, anyons located in different domains can only be connected by chains of errors that change their type when cross a DW, as in panel (d). Hence, for the X^3Z^3 code there is only one logical $\bar{X}$ consisting of Pauli-X operators only, as shown with the red string, and one logical $\bar{Z}$ dual to it. Any other logical operator will be composed of Paulis of both types, as exemplified with the green logical operator.

bound. In contrast, the existing noise-tailored version of the color code—the XYZ code—demonstrates much more modest improvements, albeit admitting interesting features such as local decoding [40]. Finding a high-threshold color code that can compete on par with the XZZX surface code at realistic noise bias would be a significant milestone in the design of fault-tolerant architectures.

In this Letter, we introduce a family of color codes tailored for the efficient correction of biased noise, which we collectively refer to as domain wall (DW) color codes. They are obtained by introducing domain walls which permute the code's excitations upon DW crossing [25]. Certain instances of these new codes demonstrate strikingly high code-capacity thresholds, matching those achievable with the noise-tailored XZZX surface code and exceeding the random-code hashing bound [41] in the regime of experimentally relevant noise parameters. In our work, we extensively explore these superior thresholds. The proposed scheme provides a means to high-threshold logical qubits and serves as a potential test bed for the experimental demonstration of the superadditivity of the coherent information [1,42–44]. Lastly, we show that various noise-tailored topological QECC studied so far—such as the XZZX surface [35] and the XYZ color [40] codes—can be formulated as instances of DW codes. Our approach hence unifies previous findings within a single framework.

The color code is a topological QECC formed by a stabilizer group $\mathcal{S}$ acting on physical qubits placed at the vertices of a trivalent, three-colorable lattice. The 6.6.6 color code is defined on a hexagonal lattice with triangular boundary conditions, as shown in Fig. 1(a). The stabilizer group $\mathcal{S}$ of the code is generated by operators associated with the faces of the lattice. Particularly, in the conventional, or the Calderbank-Shor-Steane (CSS), color code each face supports two stabilizer generators,

$$S_{\mathrm{p},f} = \prod_{v \in \partial f} X_v \quad \text{and} \quad S_{\mathrm{d},f} = \prod_{v \in \partial f} Z_v, \qquad (1)$$

which we call primal and dual stabilizers, respectively. Here, $v \in \partial f$ denotes all qubits in the support of face f and X_v, Z_v are the corresponding Pauli operators acting on qubit v. The code subspace is the $+1$ eigenvalue eigenspace of all elements of $\mathcal{S}$. One can verify from Fig. 1(a) that the code contains one more physical qubit than there are independent stabilizer generators. This remaining degree of freedom constitutes a nonlocally encoded logical qubit.

Logical operators on the color-code qubit are nontrivial strings of single-qubit Paulis which commute with code stabilizers. Identifying a string of single-qubit X operators with a logical $\bar{X}$ operator, a logical $\bar{Z}$ is derived from it by replacing X operators of the string with Zs. The correct anti-commutation relation $\{\bar{X}, \bar{Z}\} = 0$ of logical operators is guaranteed due to an odd number of qubits in their support. Alternative configurations of logical operators can be constructed by multiplying these strings with code stabilizers and, due to the CSS structure of the code, any logical $\bar{X}$ ($\bar{Z}$) operator can be implemented as a tensor

product of single-qubit X (Z) operators. As an example, the red and green strings of Fig. 1(a) are equivalent up to multiplication by the primal stabilizers of the code.

Error correction is achieved by measuring stabilizers throughout the computation. Since stringlike logical operators commute with all stabilizers, such measurements do not perturb the encoded information. By combining the information from stabilizer measurements, collectively called a syndrome, a correction can be proposed by a decoding algorithm. The performance of a QECC under an error model relies on its ability to correctly identify errors that have occurred on physical qubits and produced an observed syndrome.

The noise model we consider is independent and identically distributed across qubits. We characterize the noise model by a single-qubit error probability p and the bias $\eta = p_Z/(p_X + p_Y)$, with $p_X = p_Y$ and p_i for $i = X$, Y, Z being the probability of the corresponding error channel. With this definition, η takes values between $\eta_d = 0.5$ (depolarizing) and $\eta_{ph} = \infty$ (pure dephasing). The standard surface and color codes of the CSS type achieve their peak performance for depolarizing noise and become less efficient when dephasing prevails. To see why, consider pure dephasing noise. Since all the dual stabilizers of Eq. (1) commute with a phase-flip event, the dual syndrome indicates no information about the occurred error. Consequently, the ability of the standard surface and color codes to correct errors degrades as bias η increases.

A common strategy for improving the error correction efficiency of a code is to modify its stabilizers by applying single-qubit Clifford rotations, collectively referred to as a Clifford deformation of the code [39,45]. As an example, deforming the CSS surface code to the XZZX configuration doubles the amount of useful information associated with the dominant noise, which significantly enhances error-correcting capabilities of the code [35]. A similar deformation of the color-code stabilizers maximizes the information content of the syndrome under biased noise, resulting in a substantial gain in performance.

Our DW color code is locally equivalent to the conventional color code up to the Hadamard rotations applied to half of the qubits in the code. The DW code is therefore reminiscent of the XZZX code derived by applying the Hadamard rotation to every second qubit of the surface code [35]. An example of the DW code is shown in Fig. 1(b). Each stabilizer of weight six measures three Pauli-X and three Pauli-Z operators. Because of the structure of its stabilizers, we will refer to this instance of the DW code as the X^3Z^3 code. As shown in the figure, stabilizers of the code naturally form domain walls, separating regions where one type of Pauli is measured on each stabilizer sublattice, hence the name DW code.

To understand the advantage of the X^3Z^3 DW code over the standard color code, consider the propagation of code stabilizers flipped by Pauli errors. Flipped stabilizers are

known to obey anyonic statistics [8,14], thus we will refer to them as anyons for brevity. In the CSS code of Fig. 1(a), anyons due to Pauli-Z (X) errors can propagate in any direction within the two-dimensional lattice. Assume for instance a Z-type anyon, i.e., an anyon created by Pauli-Z errors in a primal stabilizer. Such an anyon can move freely in a 2D plane due to subsequent Z errors. Hence, the number of possible shortest-path logical operators composed of Paulis of one type is highly degenerate. In the X^3Z^3 color code, on the other hand, propagation of anyons under pure Z (or, equivalently, pure X) noise is restricted to 1D domains bounded by the DWs. This is, because the transmission of anyons through a DW requires anyons to change type [25,46,47]. Indeed, consider two stabilizers of the same color partially lying within the same domain, such as the two red stabilizers of in Fig. 1(c). Strings of single-qubit errors connecting two such anyons have to be composed of Paulis of one type. In contrast, strings connecting two anyons separated by a DW have to be composed of different Paulis, as in Fig. 1(d). Hence, at infinite bias, anyons are not permitted to cross DWs since that would require a Pauli error of a different type. The only possible logical $\bar{Z}$ operator that does not cross a DW is shown with the red string in Fig. 1(b), which is in contrast to a highly degenerate number of logical operators in the CSS code. Consequently, the probability of logical errors in the X^3Z^3 code is greatly suppressed. Since at infinite bias, the propagation of anyons is restricted to 1D domains, the decoding problem reduces to decoding a series of repetition codes, resulting in a 50% threshold. A detailed proof of this threshold is provided in Ref. [48].

Clifford transformations similar to the one described above give rise to an entire family of DW codes. We denote different instances of the DW codes as $\mathcal{DW}(\kappa, \phi)$, with the density of domain walls κ defined as the number of domain walls n_{DW} per unit distance d,

$$\kappa = \lim_{d \to \infty} \frac{n_{DW}}{d}. \tag{2}$$

The parameter ϕ denotes a clockwise rotation of DWs with respect to horizontal orientation, and the values it can take are determined by the symmetries of the code stabilizers. Using this nomenclature, the X^3Z^3 code of Fig. 1(b) corresponds to $\mathcal{DW}(1, \pi/6)$. In DW codes characterized by $\kappa \leq 1$, the dynamics of anyons at infinite bias are restricted within regions bounded by DWs, similarly to the case of the X^3Z^3 code. Such DW codes together with the XZZX code belong to a category of so-called lineon codes, i.e., codes whose anyon dynamics is restricted to quasi-1D manifolds. We will refer to DW codes with $\kappa = 1$ as the dense codes and $\kappa < 1$ as the underdense codes, with $\kappa = 0$ being the CSS code. In contrast, in codes characterized by $\kappa > 1$, DWs are placed so close to each other that anyons can propagate both along and across domains even

(a)

(b)
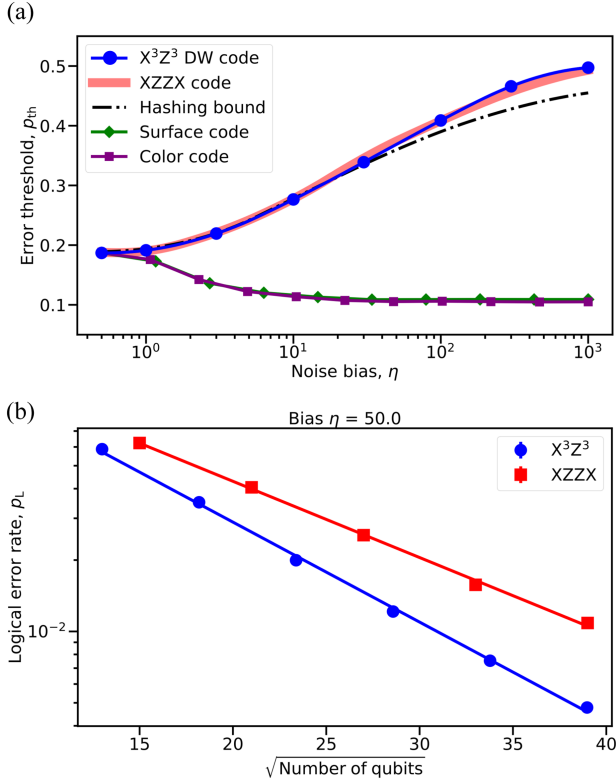
FIG. 2. (a) Code-capacity thresholds of the X^3Z^3 color (blue solid line) and the XZZX surface (thick salmon line) codes versus noise bias. For comparison, we also present the hashing bound (black dash-dotted line) and thresholds of the standard CSS surface (green diamonds) and color (purple squares) codes derived in Ref. [36]. All curves are fitted using quadratic splines for a better visual appearance. For the X^3Z^3 code, the calculated threshold values are shown explicitly with blue dots. (b) Sub-threshold logical error rates of the X^3Z^3 DW code (blue circles) and the rotated squared-shape XZZX code (red squares) calculated at bias $\eta = 50$ and single-qubit error probability $p = 25\%$.

at infinite bias. Anyon dynamics are hence not restricted to one-dimensional manifolds. We will refer to such DW codes as overdense codes, with a particularly notable example being the XYZ [40,48] color code. Anyonic excitations in such codes propagate isotropically in two dimensions, giving rise to a type-II fracton syndrome. Here, we focus on the properties of the dense X^3Z^3 code and present various alternative instances of DW codes in Ref. [48].

We numerically investigate the properties of DW codes under biased noise by performing comprehensive Monte Carlo simulations [52,53]. For decoding, we adapt the approximate maximum-likelihood decoder [36,54] and assume perfect stabilizer measurements [55]. Figure 2(a) shows the calculated code-capacity thresholds of the X^3Z^3 code at different noise biases η. Interestingly, we find that for any bias, the threshold of the X^3Z^3 color code perfectly matches that of the surface XZZX code and violates the

zero-rate hashing bound of random codes in the strong-bias regime. This observation might imply the existence of a more general theoretical upper bound that holds for non-CSS codes. We note that the hexagonal XYZ^2 code of Ref. [58] under biased noise exhibits a code-capacity threshold identical to those of the XZZX and X^3Z^3 codes, which further motivates research on what is achievable with non-CSS codes.

Below the threshold, the logical failure rates p_L of the X^3Z^3 and the square-shaped XZZX codes demonstrate qualitatively similar scaling with the number of qubits,

$$\log p_L \propto -d \propto -\sqrt{N_q}, \tag{3}$$

where N_q is the number of qubits in the code. However, we observe the X^3Z^3 code to be more resource-efficient than its surface-code counterpart, as shown in Fig. 2(b). There, we also provide a version of the X^3Z^3 code on a periodic hexagonal lattice with co-prime dimensions. We prove analytically the remarkable property of such a code at high bias: the logical failure rate scales as

$$\log p_L \propto -d^2 \propto -N_q, \tag{4}$$

similarly to the case of the co-prime XZZX code [35].

Translating the high thresholds of Fig. 2(a) into practice requires a scalable decoder, such as a commonly used one based on the matching algorithm [59–61]. To this end, we adopted a matching-based restriction decoder of Refs. [62,63] to the X^3Z^3 code. As we show in Ref. [48], error thresholds derived with the restriction decoder monotonically increase with the noise bias, however, are noticeably below the optimal thresholds, which we attribute to a nonoptimal decoding algorithm. Further improvements may be possible using more advanced versions of a matching decoder, such as the Möbius-strip decoder of Ref. [64]. We leave the question of designing optimized scalable decoders as well as fault-tolerant threshold calculations outside of the scope of this work.

Quantum error-correcting color codes are known to be more versatile than surface codes when it comes to fault-tolerant gates. Their thresholds, on the other hand, are conventionally believed to be lower than those of the surface codes for noise models other than depolarization. In this work, we have shown that the color code with a minor modification in fact demonstrates thresholds matching those achievable with tailored surface codes when qubits are subject to biased noise ubiquitous in many physical architectures. Practically, those high thresholds, accompanied by comparably resource-efficient scaling of the logical failure rate and transversality of the full Clifford gate set make the noise-tailored color codes an efficient quantum error-correcting scheme highly suitable for realistic noise.

In this work, we have considered only the simplest color code with a hexagonal layout of physical qubits. Clifford deformation into a DW-type code can be directly implemented in alternative color-code configurations. As such, a few examples of 4.8.8 DW color codes are presented in Ref. [48]. In the future, it will be important to determine the thresholds of such codes, as they typically require fewer qubits to achieve the desired failure rates and support a more diverse variety of physically distinct DW configurations due to higher-weight stabilizers. A more fundamental question is whether it is possible to impose a domain-wall structure on 3D color codes, i.e., to find a Clifford deformation that restricts propagation of anyons to lower-dimensional manifolds. The first adaptation of 3D topological codes to biased noise has very recently been reported in Ref. [65]. Such noise-tailored 3D codes, in conjunction with fault-tolerant code switching between the color codes of different dimensions, allows for transversal implementation of non-Clifford operations. Furthermore, the DW color code can be conjugated with the standard techniques for topological codes, such as magic state distillation [21,66] and entangling gates via lattice surgery [24,67,68], paving the way to a universal set of fault-tolerant gates. Combined with bias-preserving entangling gates [33,34,69,70], the logical qubit based on the DW color code becomes a promising candidate for the basic element of a universal quantum computer. On a higher level, this work reinforces the understanding that concepts from mathematical condensed matter physics are highly valuable in devising practical schemes for topological quantum error correction.

[1] M. A. Nielsen and I. L. Chuang, *Quantum Computation and Quantum Information: 10th Anniversary Edition* (Cambridge University Press, Cambridge, England, 2011).

[2] B. M. Terhal, Rev. Mod. Phys. **87**, 307 (2015).

[3] D. Gottesman, arXiv:0904.2557.

[4] S. J. Devitt, W. J. Munro, and K. Nemoto, Rep. Prog. Phys. **76**, 076001 (2013).

[5] J. Roffe, Contemp. Phys. **60**, 226 (2019).

[6] E. Knill, R. Laflamme, and W. H. Zurek, Science **279**, 342 (1998).

[7] P. Aliferis, D. Gottesman, and J. Preskill, Quantum Inf. Comput. **6**, 97 (2006).

[8] A. Y. Kitaev, Ann. Phys. (Amsterdam) **303**, 2 (2003).

[9] E. Dennis, A. Kitaev, A. Landahl, and J. Preskill, J. Math. Phys. (N.Y.) **43**, 4452 (2002).

[10] A. G. Fowler, A. C. Whiteside, and L. C. L. Hollenberg, Phys. Rev. Lett. **108**, 180501 (2012).

[11] A. G. Fowler, M. Mariantoni, J. M. Martinis, and A. N. Cleland, Phys. Rev. A **86**, 032324 (2012).

[12] H. Bombin and M. A. Martin-Delgado, Phys. Rev. Lett. **97**, 180501 (2006).

[13] A. J. Landahl, J. T. Anderson, and P. R. Rice, arXiv:1108.5738.

[14] A. M. Kubica, The ABCs of the color code: A study of topological quantum codes as toy models for fault-tolerant quantum computation and quantum phases of matter, Ph.D. thesis, California Institute of Technology, 2018.

[15] H. Bombín, New J. Phys. **17**, 083002 (2015).

[16] D. Litinski, M. S. Kesselring, J. Eisert, and F. von Oppen, Phys. Rev. X **7**, 031048 (2017).

[17] A. Kubica and M. E. Beverland, Phys. Rev. A **91**, 032330 (2015).

[18] B. Eastin and E. Knill, Phys. Rev. Lett. **102**, 110502 (2009).

[19] B. Zeng, A. Cross, and I. L. Chuang, IEEE Trans. Inf. Theory **57**, 6272 (2011).

[20] H. Bombin and M. A. Martin-Delgado, Phys. Rev. Lett. **98**, 160502 (2007).

[21] M. E. Beverland, A. Kubica, and K. M. Svore, PRX Quantum **2**, 020341 (2021).

[22] J. T. Anderson, G. Duclos-Cianci, and D. Poulin, Phys. Rev. Lett. **113**, 080501 (2014).

[23] H. Bombin and M. A. Martin-Delgado, Phys. Rev. A **76**, 012305 (2007).

[24] F. Thomsen, M. S. Kesselring, S. D. Bartlett, and B. J. Brown, arXiv:2201.07806.

[25] M. S. Kesselring, F. Pastawski, J. Eisert, and B. J. Brown, Quantum **2**, 101 (2018).

[26] A. Lavasani and M. Barkeshli, Phys. Rev. A **98**, 052319 (2018).

[27] A. J. Landahl and C. Ryan-Anderson, arXiv:1407.5103.

[28] A. G. Fowler, Phys. Rev. A **83**, 042310 (2011).

[29] P. Aliferis, F. Brito, D. P. DiVincenzo, J. Preskill, M. Steffen, and B. M. Terhal, New J. Phys. **11**, 013061 (2009).

[30] F. Brito, D. P. DiVincenzo, R. H. Koch, and M. Steffen, New J. Phys. **10**, 033027 (2008).

[31] D. Nigg, M. Müller, E. A. Martinez, P. Schindler, M. Hennrich, T. Monz, M. A. Martin-Delgado, and R. Blatt, Science **345**, 302 (2014).

[32] M. D. Shulman, O. E. Dial, S. P. Harvey, H. Bluhm, V. Umansky, and A. Yacoby, Science **336**, 202 (2012).

[33] J. Guillaud and M. Mirrahimi, Phys. Rev. X **9**, 041053 (2019).

[34] A. S. Darmawan, B. J. Brown, A. L. Grimsmo, D. K. Tuckett, and S. Puri, PRX Quantum **2**, 030345 (2021).

[35] J. P. B. Ataides, D. K. Tuckett, S. D. Bartlett, S. T. Flammia, and B. J. Brown, Nat. Commun. **12**, 2172 (2021).

[36] D. K. Tuckett, A. S. Darmawan, C. T. Chubb, S. Bravyi, S. D. Bartlett, and S. T. Flammia, Phys. Rev. X **9**, 041031 (2019).

[37] D. K. Tuckett, S. D. Bartlett, and S. T. Flammia, Phys. Rev. Lett. **120**, 050505 (2018).

[38] D. K. Tuckett, S. D. Bartlett, S. T. Flammia, and B. J. Brown, Phys. Rev. Lett. **124**, 130501 (2020).

[39] K. Tiurev, P.-J. H. S. Derks, J. Roffe, J. Eisert, and J.-M. Reiner, Quantum **7,** 1123 (2023).

[40] J. F. S. Miguel, D. J. Williamson, and B. J. Brown, Quantum **7,** 940 (2023).

[41] C. H. Bennett, D. P. DiVincenzo, J. A. Smolin, and W. K. Wootters, Phys. Rev. A **54,** 3824 (1996).

[42] J. Fern and K. B. Whaley, Phys. Rev. A **78,** 062335 (2008).

[43] J. Bausch and F. Leditzky, SIAM J. Comput. **50,** 1410 (2021).

[44] G. Smith and J. Yard, Science **321,** 1812 (2008).

[45] A. Dua, A. Kubica, L. Jiang, S. T. Flammia, and M. J. Gullans, PRX Quantum **5,** 010347 (2024).

[46] M. S. Kesselring, J. C. Magdalena de la Fuente, F. Thomsen, J. Eisert, S. D. Bartlett, and B. J. Brown, PRX Quantum **5,** 010342 (2024).

[47] J. C. Magdalena de la Fuente, J. Eisert, and A. Bauer, J. Math. Phys. (N.Y.) **64,** 111904 (2023).

[48] See Supplemental Material at http://link.aps.org/supplemental/10.1103/PhysRevLett.133.110601, which includes Refs. [49–51] for details.

[49] B. J. Brown and D. J. Williamson, Phys. Rev. Res. **2,** 013303 (2020).

[50] R. M. Karp, in *Complexity of Computer Computations* (Springer, New York, 1972), pp. 85–103.

[51] J. W. Harrington, Analysis of quantum error-correcting codes: Symplectic lattice codes and toric codes, Ph.D. thesis, California Institute of Technology, 2004.

[52] D. K. Tuckett, Tailoring surface codes: Improvements in quantum error correction with biased noise, Ph.D. thesis, University of Sydney (2020) [qecsim: https://github.com/qecsim/qecsim].

[53] The codes used for numerical simulations of the QECCs studied in this work and the simulation data are available at https://github.com/HQSquantumsimulations/domain-wall-code-published.

[54] S. Bravyi, M. Suchara, and A. Vargo, Phys. Rev. A **90,** 032326 (2014).

[55] For alternative decoders for color codes, see Refs. [56,57].

[56] H. G. Katzgraber, H. Bombin, and M. A. Martin-Delgado, Phys. Rev. Lett. **103,** 090501 (2009).

[57] L. Berent, L. Burgholzer, P.-J. H. S. Derks, J. Eisert, and R. Wille, arXiv:2303.14237.

[58] B. Srivastava, A. F. Kockum, and M. Granath, Quantum **6,** 698 (2022).

[59] J. Edmonds, Can. J. Math. **17,** 449 (1965).

[60] O. Higgott, ACM Trans. Quantum Comput. **3,** 1 (2022).

[61] B. J. Brown, IEEE BITS Inf. Theory Mag. **2,** 5 (2022).

[62] N. Delfosse, Phys. Rev. A **89,** 012317 (2014).

[63] C. Chamberland, A. Kubica, T. J. Yoder, and G. Zhu, New J. Phys. **22,** 023019 (2020).

[64] K. Sahay and B. J. Brown, PRX Quantum **3,** 010310 (2022).

[65] E. Huang, A. Pesah, C. T. Chubb, M. Vasmer, and A. Dua, PRX Quantum **4,** 030338 (2023).

[66] S. Bravyi and A. Kitaev, Phys. Rev. A **71,** 022316 (2005).

[67] D. Horsman, A. G. Fowler, S. Devitt, and R. V. Meter, New J. Phys. **14,** 123011 (2012).

[68] A. J. Landahl and C. Ryan-Anderson, arXiv:1407.5103.

[69] S. Puri, L. St-Jean, J. A. Gross, A. Grimm, N. E. Frattini, P. S. Iyer, A. Krishna, S. Touzard, L. Jiang, A. Blais, S. T. Flammia, and S. M. Girvin, Sci. Adv. **6,** eaay5901 (2020).

[70] Q. Xu, J. K. Iverson, F. G. S. L. Brandão, and L. Jiang, Phys. Rev. Res. **4,** 013082 (2022).

[71] L. Bennett, B. Melchers, and B. Proppe, Curta: A general-purpose high-performance computer at ZEDAT, Freie Universität Berlin (2020).